Available online at www.sciencedirect.com
ScienceDirect
Russian Geology and Geophysics 50 (2009) 222–233
RUSSIAN GEOLOGY AND GEOPHYSICS
www.elsevier.com/locate/rgg

Applying the transmission line theory to study ungrounded horizontal loop self-transients

N.O. Kozhevnikov*

Trofimuk Institute of Petroleum Geology and Geophysics, Siberian Branch of the RAS, 3 prosp. Akad. Koptyuga, Novosibirsk, 630090, Russia

Received 7 February 2008; accepted 24 September 2008

Abstract

Ungrounded horizontal loop responses at low frequencies and/or late times can be modeled in terms of an equivalent circuit with lumped elements, but a loop in a general case is a distributed system. At high frequencies and/or early times, the wire in combination with the underlying earth makes a transmission line in which current behaves according to the wave equation. Solving the equation for current turn-off is quite difficult because the primary parameters of the wire–earth system depend, in an intricate way, on earth conductivity (resistivity) and frequency (or time). In modeling the current turn-off process, the loop was simulated as a symmetrical combination of two identical transmission lines with shorted outputs. Modeling was performed in the frequency domain with subsequent transformation into the time domain. Comparison of measured and computed transient self responses showed that good fit requires taking into account (1) interaction of each line with its own image current, (2) mutual inductance of the two lines, and (3) skin effect in the wire. As a result of mutual inductance, the parameters of the lines and, hence, of the whole loop depend on local conductivity, which, at least in principle, may allow one to infer the resistivity of shallow subsurface from current turn-off responses. A real ungrounded horizontal loops lacks symmetry at early times and its magnetic field differs from that predicted by the conventional methods of induction soundings.

Keywords: TEM method; ungrounded loop; current turn-off; wave equation; transmission line

Introduction

Ungrounded horizontal loops are used in electromagnetic surveys to excite the primary field and to measure the secondary magnetic field. They are the usual basic constituents of measurement systems in TEM prospecting and sounding. Inasmuch as the measured responses of the earth are convolved with the transmitter and receiver loop responses, one has to take into account the features and time of transmitter current turn-off as well as the receiver self response in both forward and inverse modeling (Efimov, 1976; Kozhevnikov and Plotnikov, 2004; Sokolov et al., 1978; Vishnyakov and Vishnyakova, 1974; Zakharkin, 1981).

In studying the self-response of a loop (Fig. 1, *a*) in frequency and/or time domain, the loop is simulated by an equivalent circuit (Fig. 1, *b*) with lumped inductance (L_0), capacitance (C_0), and resistance R_0 (Efimov, 1976; Hayles and Sinha, 1986; Kozhevnikov and Plotnikov, 2004; Qian, 1985; Nikolaev et al., 1988; Vishnyakov and Vishnyakova, 1974; Zakharkin, 1981). The loop inertia is commonly expressed via the resonance frequency f_0 given by

$$f_0 = \frac{1}{2\pi\sqrt{L_0 C_0}}. \quad (1)$$

The equivalent loop elements are as a rule defined as $R_0 = R{\cdot}P$, $L_0 = L{\cdot}P$, and $C_0 = C{\cdot}P$, where R, L, and C are the wire resistance, inductance, and capacitance per unit length, and P is the loop perimeter (Veshev, 1980; Zakharkin, 1981). Thus, (1) becomes

$$f_0 = \frac{1}{2\pi P\sqrt{LC}}, \quad (2)$$

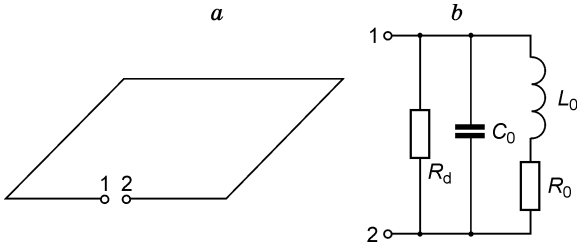

Fig. 1. Ungrounded horizontal loop (*a*) and equivalent lumped circuit (*b*).

* Corresponding author.
E-mail address: KozhevnikovNO@ipgg.nsc.ru (N.O. Kozhevnikov)

1068-7971/$ - see front matter © 2009, IGM, Siberian Branch of the RAS. Published by Elsevier B.V. All rights reserved.
doi:10.1016/j.rgg.2008.09.004

where from the size dependence of loop resonance frequency becomes evident.

In addition to the elements of the loop itself, Figure 1, *b* shows an external damping resistor load, with the resistance R_d, connected to the loop output. The resistor R_d suppresses high-frequency ringing which appears in the loop when it becomes electronically switched off (from a battery or a dc power unit). The optimal value R_d is given by

$$R_d = \frac{1}{2}\sqrt{\frac{L}{C}}. \quad (3)$$

When such a resistor becomes connected to the loop, the latter operates in a so-called critical state corresponding to the least duration of the transient self response of the loop (Efimov, 1976; Vishnyakov and Vishnyakova, 1974).

The equivalent lumped circuit model allows estimating the loop resonance frequency, the form, and length of current cutoff, minimum allowable recording time, and dynamic measurement errors due to departure of the loop parameters from the ideal values, which is essential in engineering practice.

Early-time TEM measurements are becoming of ever greater importance in near-surface surveys through recent 10–15 years. Shorter initial recording time requires a shorter duration of transmitter current turn-off. Yet, this way has technological and basic limitations. The latter are, namely, that the lumped-circuit model fails to account for empirical data (Kozhevnikov and Nikiforov, 1998, 2000; Kozhevnikov, 2006) because at early times the wire combined with the underlying ground make a system with distributed parameters. According to comparison of loop input resistance computed using the lumped-circuit model with the values measured at different frequencies, the loop behaves as a typical long transmission line at high frequencies and, respectively, early times (Kozhevnikov and Nikiforov, 1998, 2000; Kozhevnikov, 2006).

A loop model as a combination of two transmission lines

A transmission line made of a wire and the ground it lies on seems to have little in common with an ungrounded horizontal loop. However, by symmetry, a loop can be presented as two serially connected identical transmission lines with their meeting common point grounded. The current/voltage source likewise can be simulated by a combination of identical serially connected sources with a grounded common point.

See a square loop, with a wire of the length *P*, lying on the ground and a current (voltage) source in Fig. 2, *a*, and the loop and the source presented as two identical transmission lines of the length *P*/2 each in Fig. 2, *b*. Circled 2 in Fig. 2, *a* denotes the source with the output voltage *U* and the internal resistance R_i, and circled 3 in Fig. 2, *b* marks two sources with the output voltage *U*/2 and the self resistance R_i/2 each.

Using two sources equal in their effect to the original source ensures complete symmetry (Fig. 2, *b*) and is advantageous over an equivalent lumped-circuit model with two identical four-poles of Nakhabtsev et al. (1985) which represents the voltage source as a single unit and is difficult for analysis. The system in Fig. 2, *b* being symmetrical, the point *O* and the point at the distance *P*/2 from it have the same potential, and their connection to the earth causes no effect on the distribution of voltage and current in the loop. Therefore, one can use a wire of the length $l = P/2$ shorted at the output to simulate the responses of an ungrounded loop of the perimeter *P* (Fig. 2, *c*).

It is hard to study the operation of this line in all details with regard to frequency dependence of its parameters and to the ground properties, but some relatively simple cases may be instructive. For instance, simulating the loop as a system with distributed elements provides a general idea of current turn-off after the loop ends have being electronically switched off. Consider a practically important case of high-frequency (f_0) ringing in an open loop ($R_d = \infty$) left alone after being switched off.

Let one loop end be the origin point, and the distance from this end along the wire be the *x* coordinate; then, the *x* coordinate of the other end corresponds to the loop perimeter *P*. Let the steady current in the loop be I_0. The behavior of the current $I(t, x)$ in the wire–earth system after the loop has been switched off is given by (Kozhevnikov and Nikiforov, 1998, 2000; Kozhevnikov, 2006)

$$\frac{\partial^2 I}{\partial t^2} - \frac{1}{LC}\frac{\partial^2 I}{\partial x^2} + \left(\frac{R}{L} + \frac{G}{C}\right)\frac{\partial I}{\partial t} + \frac{GR}{LC}I = 0 \quad (4)$$

with the boundary ($I(t, 0) = I(t, P) = 0$) and initial ($I(0, x) = I_0$, $\partial I(0, x)/\partial t = 0$) conditions; *G* is the wire insulation conductance per unit length. Taking into account that

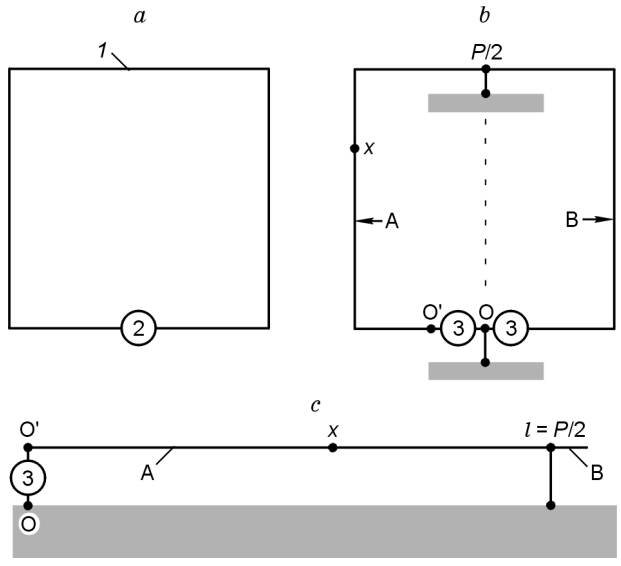

Fig. 2. Ungrounded horizontal loop 1 and current source 2 (*a*); same loop and current source presented as two identical transmission lines A, B and sources 3 (*b*); output-shorted line of length $l = P/2$ (*c*).

$(G/C) \ll (R/L)$ and neglecting the last term in (4) because the loop has a high resonant frequency, we obtain

$$\frac{\partial^2 I}{\partial t^2} - \frac{1}{LC}\frac{\partial^2 I}{\partial x^2} + \frac{R}{L}\frac{\partial I}{\partial t} = 0. \quad (5)$$

Using known solutions, e.g., for decaying string oscillations (Aramanovich and Levin, 1969), it is easy to show that, with the above assumptions, the solution of (5) is the sum

$$I(x, t) =$$

$$I_0 \frac{4}{\pi} \sum_{k=0}^{\infty} \frac{1}{2k+1} e^{-mt} \left(\cos \omega_k t + \frac{m_k}{\omega_k} \sin \omega_k t \right) \sin \frac{\pi x (2k+1)}{P}. \quad (6)$$

According to (6), switch-off produces current standing waves in the loop, with the wavelength of the k-th wave $\lambda_k = (2P)/(2k + 1)$, and the angular frequency

$$\omega_k = \left[(2k+1)^2 (\pi a/P)^2 - m^2 \right]^{1/2}, \quad (7)$$

where $a = (LC)^{-1/2}$, $m = R/2L$. The amplitude of each standing wave decays exponentially with the time constant

$$\tau_0 = 1/m = 2L/R.$$

The phase velocity of the traveling wave, and the period and wavelength of the standing wave are related as $\lambda = \nu/f$. Inasmuch as $\nu = (LC)^{-1/2}$ at high frequencies (Simonyi, 1956; Johnson and Graham, 2003), the loop resonance frequency is

$$f_0 = \frac{\nu}{2P} = \frac{1}{2P\sqrt{LC}}. \quad (8)$$

The result differs from that predicted by the lumped-circuit model: the loop resonance frequency according to (8) is π times the frequency calculated with (2). The main mode frequency f_0 can be found from (7) for ω_k assuming $k = 0$ and taking into account that, at high frequencies, the second term in brackets is small compared with the first term.

To see what happens at different points of the wire after the loop has been switched off, one can present the current turn-off process as a superposition of forward and reflected waves in a transmission line formed of a wire and the underlying ground (Fig. 3, *a*). Switch-off produces, in each of the two transmission lines, a negative current wave (step) which is equal in amplitude to the pre-disconnection current and travels from the loop input to the symmetry point ($x = P/2$). As this wave reaches the zero-potential (pseudo-grounded) midpoint, there arises a reflected wave traveling from the midpoint back to the input. The total current in the line is the sum of the pre-turnoff steady current and two waves traveling, respectively, from the loop input to the midpoint and back. The reflected wave reflects again from the open loop input, and since then the current in the wire becomes a sum of three waves and steady current. Then other reflections occur, the superposition of waves traveling forward and back produces a standing wave, and the process becomes periodical. It would continue for an infinitely long time in an ideal transmission line but real lines are always lossy thus making the standing waves attenuate with time.

By the lag effect, the primary magnetic field in the wire–earth system at earliest times (microseconds for 100 m × 100 m loops) differs from that predicted by the classical theory of EM prospecting. The early-time current distribution in the loop is symmetrical about the y axis but lacks symmetry about the x axis (Fig. 3, *a*). Therefore, the loop transient and/or frequency responses may, in principle, depend on the place of transmitter connection in the case of an asymmetrical environment (e.g., a loop laid on an electrically asymmetrical earth). This effect is known in the theory and practice of near-surface antennas (Lavrov and Knyazev, 1965).

To stop the turn-off process, one has to provide resistance matching, or the conditions when there is no reflection from the open loop input. Matching can be achieved with an external resistor (R_d), connected to the loop input, equal to double high-frequency characteristic impedance Z_w of the wire–earth line, which is $2Z_w = 350$ Ohm in a standard copper wire, with a section of a few mm^2, laid on the ground (Kozhevnikov and Nikoforov, 1998, 2000; Kozhevnikov, 2006). According to the long transmission line theory, the high-frequency impedance is loss independent but is a function of line per-unit-length inductance and capacitance $Z_w = \sqrt{L/C}$ (Johnson and Graham, 2003; Simonyi, 1956). Therefore, the resistance intended to suppress current oscillations in the loop should be $2\sqrt{L/C}$. This value is independent of the loop size and is four times that calculated by (3) for an equivalent distributed circuit.

Of course, the parameters of a real transmission line do depend on frequency/time, the earth-induced frequency dispersion being especially high for the resistance (see below). If the frequency/time dependence of R is impossible to neglect, one has to use the equation (Kozhevnikov, 2006)

$$\frac{\partial^2 I}{\partial t^2} - \frac{1}{LC}\frac{\partial^2 I}{\partial x^2} + \frac{1}{L}\int_0^t R(\tau)\frac{\partial I(t-\tau)}{\partial t} d\tau = 0 \quad (9)$$

instead of (5).

Solving (9) is a tough problem in a general case, but it is physically reasonable to assume that the solution is presentable as a sum of standing waves of the base and higher frequencies. As the wire active resistance increases proportionally to frequency (see below), waves with large k attenuate rapidly, and in a few microseconds only the base mode survives in the wire–earth system of the $\lambda_0 = 2P$ standing wave (Fig. 3, *b*), with a current node and a voltage antinode at input points 1 and 2 and a current antinode and a voltage node at point 3.

The above equations and considerations give a generalized idea of the early-time current distribution along the loop wire. The next step is obviously to check the model predictions against field measurements. The available TEM data amenable to interpretation in terms of a distributed-circuit model can be summarized as follows.

(1) Loop input impedance depends on frequency in the same way as the input impedance of a transmission line

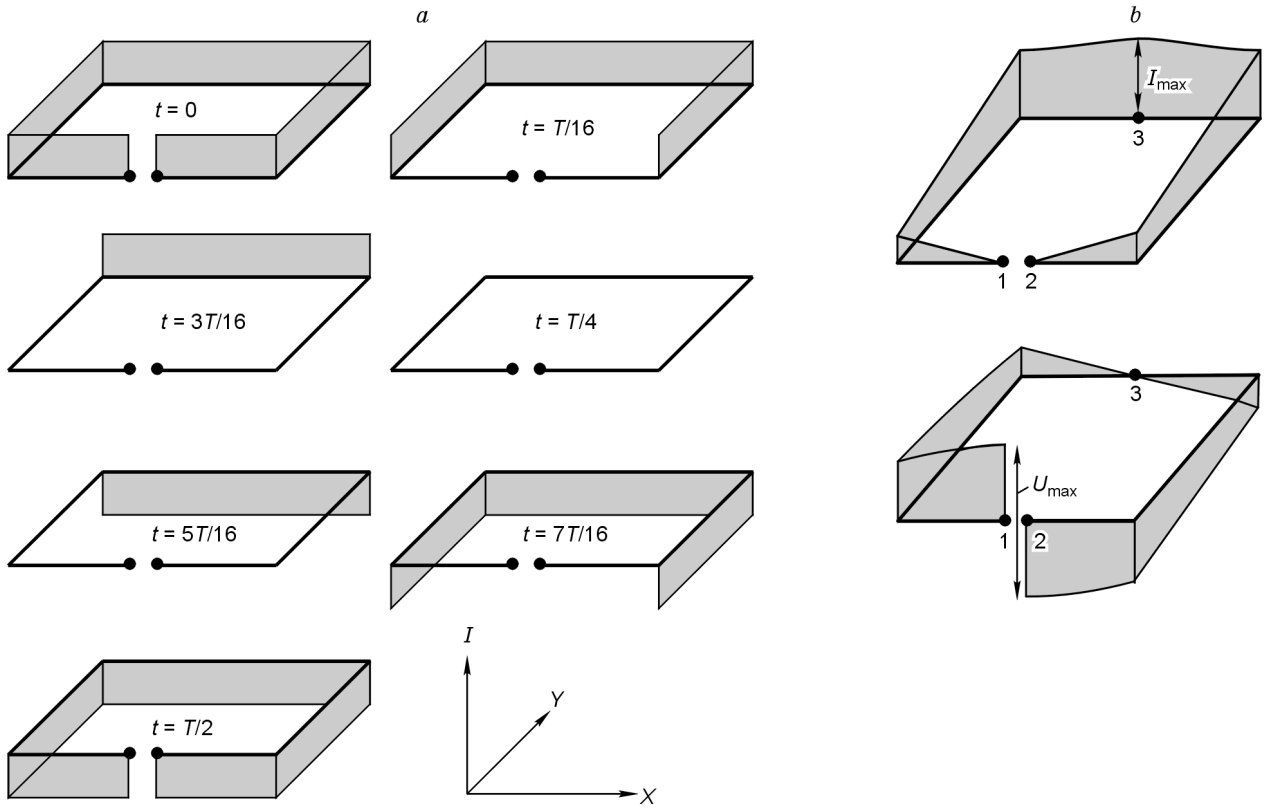

Fig. 3. Snapshots of current distribution in loop after current turn-off (*a*); current and voltage standing waves in loop, main mode (*b*). *T* is period of main mode. Current distribution and primary magnetic field are symmetrical about *y* axis but asymmetrical about *x* axis.

shorted at the output (Kozhevnikov and Nikiforov, 1998, 2000; Kozhevnikov, 2006).

(2) Switch-off gives rise to attenuating current and voltage standing waves in an open loop (Helwig and Kozhevnikov, 2003; Kozhevnikov and Nikiforov, 1998, 2000; Kozhevnikov, 2006).

(3) A matching resistor connected to the loop input causes a delay in the stepwise current turn-off which is proportional to the distance from the loop input terminals (Helwig and Kozhevnikov, 2003) instead of synchronous or synphase turn-off.

This study is an attempt to interpret "quantitatively" the experimental data for point (2) using the model of Fig. 2.

The existence of standing waves in an ungrounded horizontal loop was recorded at different points of the wire. Excitation was by a battery, a current-limiting resistor $R_{c\text{-}l}$, and a fast electronic switch connected in series (Fig. 4, *a*), and switch-off caused current oscillations.

See Fig. 4, *b–d* for field data from the Ol'khon test site (western shore of Lake Baikal) of the Irkutsk Technical University measured with a 200 m by 200 m loop of a standard geophysical copper wire. Current oscillations were measured with an oscilloscope and a low-resistance resistor shunt connected to the wire break immediately at one input end ($x = 0$), at the distance $x = 0.25P$ from it, and at the midpoint ($x = 0.5P$). The current decay differed at the three points (Fig. 4, *b–d*), i.e., at early times (and, respectively, high frequencies), the loop behaved as a distributed circuit. The amplitude of current oscillations was maximum at the midpoint and zero at the input where the battery was connected. Thus, there were indeed current nodes at the loop input and a current antinode at the midpoint. The current oscillation amplitudes at the points $x = 0$, $x = 0.25$, and $x = 0.5$ are in the proportion predicted by (6) for the base standing current wave.

Comparison of measured and computed data

The loop model is used below to compute the transients and to compare them with the measured responses. First one has to choose the modeling strategy. Solving (9) is hard and, moreover, it may be difficult to formulate the boundary and initial conditions for the case of loop shunting with a matching resistor, not to mention a circuit element with complex frequency-dependent impedance.

Mind that at high frequencies and, correspondingly at early times, one can model the responses of an ungrounded loop with the perimeter *P* in terms of a single-wire transmission line of the length $l = P/2$ shorted at the output. There is much literature on *frequency-domain* modeling of these lines (e.g., Baskakov, 1980; Johnson and Graham, 2003; Simonyi, 1956). Thus it appears reasonable to find first a frequency-domain solution, using the transmission line theory, and then to transform it into the time domain. Note also that the external elements which may be connected at the loop input or at any

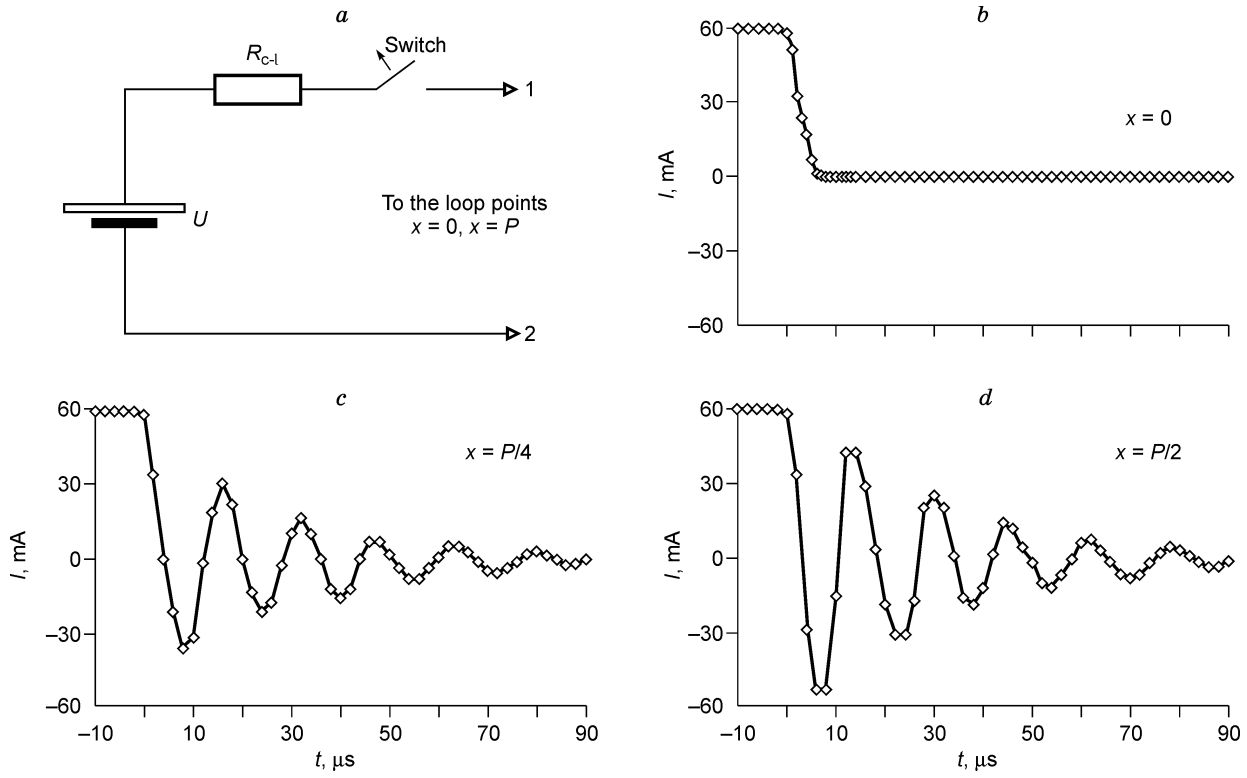

Fig. 4. Circuit producing current pulses in loop (*a*) and current oscillations (*b–d*) measured at different loop points after switch off.

other point of the wire, including frequency-dependent ones, are easily taken into account in the frequency domain.

Before proceeding to analysis of a loop with the perimeter P as a system consisting of halves each being presented as an output-shorted single-wire transmission line of the length $l = P/2$, it is pertinent to give a synopsis of the theory of transmission lines.

In the theory and practice of transmission lines, the knowledge of the propagation constant $\dot{\gamma}$ and the characteristic impedance $\dot{Z}_{\rm w}$., which in the general case are complex and frequency-dependent, provides an exhaustive description of the line in terms of the chosen model. The propagation constant $\dot{\gamma}$ is

$$\dot{\gamma} = \alpha + j\beta,$$

where α is the attenuation constant and β is the phase constant, both of the same dimension 1/m, $j = \sqrt{-1}$.

The per-unit-length parameters (capacitance, resistance, and shunt conductance) being known, α and β are found as (Baskakov, 1980; Simonyi, 1956):

$$\alpha = \left\{\frac{1}{2}\left(RC - \omega^2 LC\right) + \frac{1}{2}\left[\left(R^2 + \omega^2 L^2\right)\left(G^2 + \omega^2 C^2\right)\right]^{1/2}\right\}^{1/2},$$

$$\beta = \left\{\frac{1}{2}\left(\omega^2 LC - RG\right) + \frac{1}{2}\left[\left(R^2 + \omega^2 L^2\right)\left(G^2 + \omega^2 C^2\right)\right]^{1/2}\right\}^{1/2},$$

It is convenient to write the impedance $\dot{Z}$ as a product of its modulus value and the phase constant:

$$\dot{Z}_{\rm w} = Z_0 e^{j\psi},$$

where

$$Z_0 = \left(\frac{R^2 + \omega^2 L^2}{G^2 + \omega^2 C^2}\right)^{1/4},$$

$$\psi = \arg \dot{Z}_{\rm w} = \frac{1}{2} \arctan \frac{G/(\omega C) - R/(\omega L)}{1 + (GR)/(\omega^2 LC)}.$$

See Fig. 5, *a* for a wire of the length $P/2$ which, combined with the ground under it, makes up a single-wire transmission line. Let the origin of the x axis be at the left end of the wire, where the input voltage ($\dot{U}_1$) and current ($\dot{I}_1$) complex amplitudes are specified. For the right end, specified are the output voltage (U_2) and current ($\dot{I}_2$). This system is a linear stationary four-pole described by the respective matrix, according to the general theory of electrical circuits.

For the line in Fig. 5, *a*, the input ($x = 0$) and output ($x = l$) currents and voltages are related as (Baskakov, 1980):

$$\dot{U}_1 = \dot{U}_2 \cosh \dot{\gamma} l + \dot{I}_2 Z_{\rm w} \sinh \dot{\gamma} l,$$

$$\dot{I}_1 = \frac{\dot{U}_2}{\dot{Z}_{\rm w}} \sinh \dot{\gamma} l + \dot{I}_2 \cosh \dot{\gamma} l.$$

The complex voltage and current amplitudes at any point are expressed via $\dot{U}_2$ and $\dot{I}_2$ as

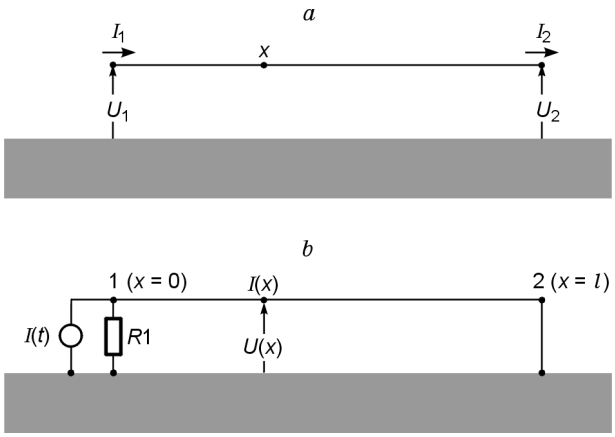

Fig. 5. Segment of a transmission line consisting of loop wire and underlying ground (*a*); one of two lines of length $l = P/2$ (Fig. 2): output is shorted and a current source and a resistor are connected to input (*b*).

$$\dot{U}(x) = \frac{\dot{U}_2 + \dot{I}_2\dot{Z}_w}{2} e^{\dot{\gamma}(l-x)} + \frac{\dot{U}_2 - \dot{I}_2\dot{Z}_w}{2} e^{-\dot{\gamma}(l-x)}, \quad (10)$$

$$\dot{I}(x) = \frac{\dot{U}_2 + \dot{I}_2\dot{Z}_w}{2\dot{Z}_w} e^{\dot{\gamma}(l-x)} - \frac{\dot{U}_2 - \dot{I}_2\dot{Z}_w}{2\dot{Z}_w} e^{-\dot{\gamma}(l-x)}, \quad (11)$$

Figure 5, *b* shows a loop half presented as an output-shorted single-wire transmission line of the length $l = P/2$ and the matching resistor $R1$ intended to prevent free current and voltage oscillations in the line. It is obvious that $R1 = R_d/2$, where R_d is the resistor connected to the loop input end (Fig. 1, *b*).

In the frequency domain, the system in Fig. 5, *b* consisting of a wire, ground under it, and the resistor $R1$, is described by a complex transfer function $\dot{S}(\omega)$ written as the output/input current ratio:

$$\dot{S}(\omega) = \frac{\dot{I}(x, \omega)}{\dot{I}(0, \omega)}, \; x \in [0, l]. \quad (12)$$

Using (10) and (11) and taking into account that (i) $U(P/2) = 0$ for an output-shorted line and (ii) the line resistance at zero frequency equals the dc resistance of a wire of the length $l = P/2$, this ratio at $\omega = 0$ is found as

$$\dot{S}(0) = \frac{R1}{R(0)l + R1}.$$

If the frequency is nonzero,

$$\dot{S}(\omega) = \frac{R1}{\dot{Z}_{in} + R1} \cdot \frac{e^{\dot{\gamma}(l-x)} + e^{-\dot{\gamma}(l-x)}}{e^{\dot{\gamma}l} + e^{-\dot{\gamma}l}},$$

where $\dot{Z}_{in}$ is the line input impedance. For an output-shorted line (Baskakov, 1980; Johnson and Graham, 2003),

$$\dot{Z}_{in} = \dot{Z}_w \tanh(\dot{\gamma}l).$$

To move on, one has to specify $\dot{I}(x, \omega)$ and the model in which R, L, C, and G are frequency-dependent and also depend on the wire material and geometry, and on earth's resistivity.

Transmitter current pulses are normally produced by a periodic on/off switch of a battery or a dc generator (Fig. 4, *a*). At switch off, the *input* current almost instantaneously zeroes and holds zero until switch on. Thus, one can assume that an ideal current source is connected to the input of the transmission line when studying loop responses over the switch-off time interval.

Let a series of square current pulses (I_1) with the period T form at the input of the wire–earth transmission line, with the amplitudes I_0, and let the zero time coincide with the trail of one of the pulses. Then the input current, at the point $x = 0$ (Fig. 5, *b*), can be written as a Fourier series (Simonyi, 1956):

$$I_1(t) = I_0\left\{\frac{1}{2} - \frac{2}{\pi}\sum_{k=1}^{\infty}\frac{1}{2k-1}\sin(2k-1)\frac{2\pi}{T}t\right\}.$$

If the complex transfer function of the transmission line (12) is written as

$$\dot{S}(\omega) = S(\omega)\cdot e^{j\varphi(\omega)},$$

where $S(\omega)$ and $\varphi(\omega)$ are the amplitude and phase of $\dot{S}(\omega)$, respectively, the output current will be

$$I_2(t) = I_0\left\{\frac{S(0)}{2} - \frac{2}{\pi}\sum_{k=1}^{\infty}\frac{1}{2k-1}S\left[(2k-1)\frac{2\pi}{T}\right]\times \right.$$
$$\left.\sin\left\{(2k-1)\frac{2\pi}{T}t + \varphi\left[(2k-1)\frac{2\pi}{T}\right]\right\}\right\}. \quad (13)$$

To calculate the complex transfer function, with its amplitude and phases included in (13), one has to know the parameters of the wire–earth line. Per-unit-length parameters of transmission lines used in induction surveys are discussed in (Alekseev et al., 1978; Alekseev and Yakovlev, 1982; Evdokimov et al., 1974; Nakhabtsev et al., 1985; Veshev, 1980; Veshev et al., 1974). The line parameters have been assumed frequency-independent in this study, but their frequency dependence and the ground resistivity should be taken into account when modeling real systems.

The capacitance (C) can be estimated as follows. The ground surface is equipotential with respect to the wire electric field, and the capacitance of a horizontal wire laid at the height h above the conductive ground can be found using the image method (Fig. 6, *a*). As a result, one arrives at the known equation (Bazutkin and Dmokhovskaya, 1983):

$$C, \text{ F/m} = \varepsilon\frac{10^{-9}}{18\ln(2h/r)}, \quad (14)$$

where r is the wire radius and ε is the relative permittivity of the wire environment. When (14) is applied to estimate the capacitance of geophysical lines, ε is taken as some effective value ε_{ef} in a range between relative permittivities of air and insulating material.

The capacitance of a horizontal wire plotted as a function of its height in Fig. 6, *b* was calculated using (14) for wires with the commonly used radiuses r = 0.5, 1, and 2 mm,

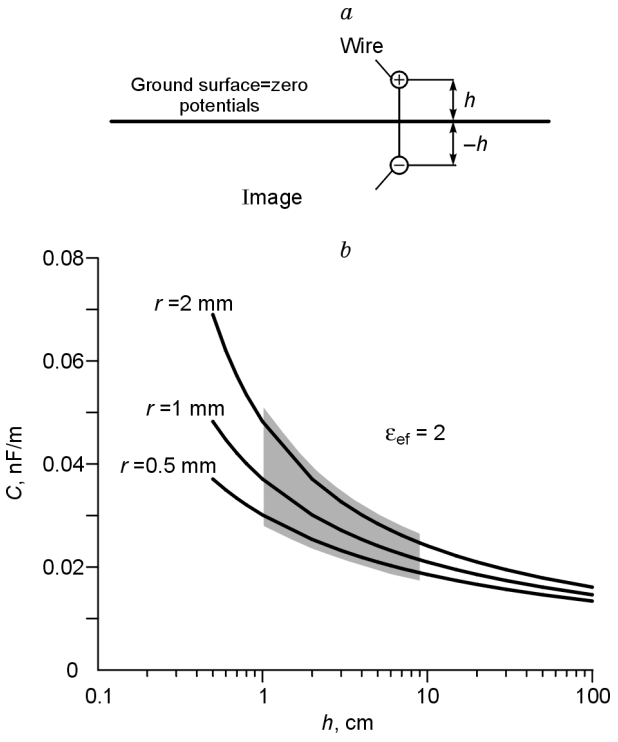

Fig. 6. Wire and its image for electric field (*a*); wire capacitance as a function of its radius and height above ground surface (*b*).

assuming $\varepsilon_{ef} = 2$. Thus, the capacitance of a wire laid near the ground surface depends on the height h: it becomes 2 times lower as h increases from 1 to 10 cm (gray zone in Fig. 6). Precise C determination makes no sense because the wire lies on a real surface with its variable topography, vegetation, and moisture, but (14), nevertheless, provides reasonable capacitance estimates depending on the wire parameters and height.

Unlike the capacitance, the inductance and resistance per unit length are frequency-dependent. A current change in a wire near the surface induces current to flow in the earth. If the earth behaves as an electrically uniform half-space, this current produces the same magnetic field as it would be by the mirror image of wire current. The effective depth h_{ef} of the image current depends on the subsurface skin depth δ:

$$h_{ef} = \delta = \sqrt{2/(\sigma\omega\mu)},$$

where σ and μ are the earth conductivity and magnetic permeability, respectively, and ω is the current angular frequency. Therefore, the zero planes for voltage and current do not coincide: for the former it is at the ground surface (Fig. 6, *a*), but for the latter it is selected to lie on midway between the magnetically equivalent image current below (at h_1) and the real wire current above (Fig. 7, *a*).

Then, the wire complex impedance (per unit length) is given by (Wang and Liu, 2001)

$$\dot{Z}_{wr} = R_{wr} + j\omega\frac{\mu_0}{2\pi}\ln\frac{2(h+p)}{r}, \qquad (15)$$

where R_{wr} is the resistance of a wire itself, and $p = \delta(2j)^{-1/2}$. The second term in (15) accounts for return or image current in conductive earth.

At high frequencies, the skin effect in a wire influences its resistance, and this influence can be included as follows (Simonyi, 1956):

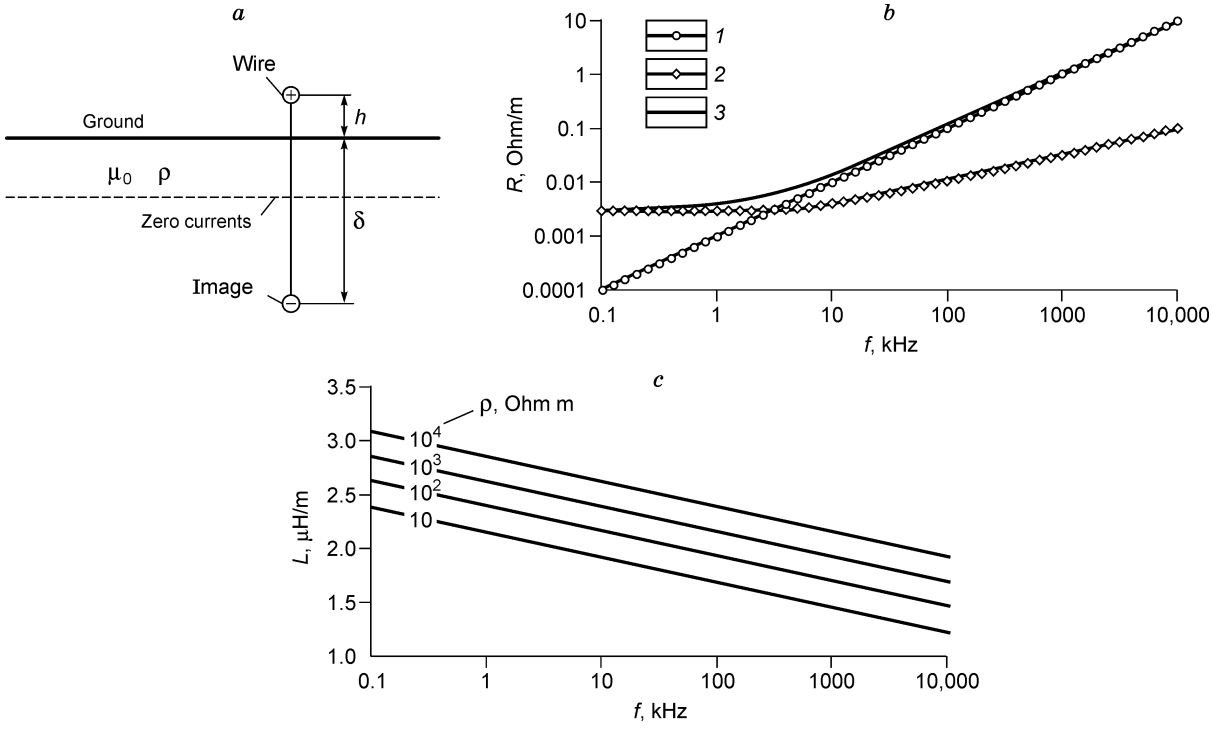

Fig. 7. Wire and its image for magnetic field (*a*); frequency dependence of wire resistance (*b*); wire inductance as a function of frequency and earth resistivity (*c*), due to skin effect in earth (*1*), skin effect in wire (*2*), both in earth and wire (*3*).

$$R_{wr} = R_{dc}\left(1 + \frac{\theta^4}{3}\right) \text{ for } \theta < 1, \quad (16a)$$

$$R_{wr} = R_{dc}\left(\theta + \frac{1}{4} + \frac{3}{64\theta}\right) \text{ for } \theta > 1, \quad (16b)$$

where R_{dc} is the dc wire resistance; $\theta = r/(2\delta_{wr})$; $\delta_{wr} = \sqrt{2/(\omega\mu_{wr}\sigma_{wr})}$; μ_{wr} is the magnetic permeability of the wire and σ_{wr} is the conductivity of its material. For $\theta = 1$ R_{wr} was calculated as a mean of two values found by (16a and b).

The wire resistance and inductance per unit length, with regard to current in the earth and the skin effect in the wire are

$$R_1 = R_{wr} + \mathrm{Re}\dot{Z}_{wr}, \quad (17)$$

$$L_1 = \frac{\mathrm{Im}\dot{Z}_{wr}}{j\omega}. \quad (18)$$

The skin effect is known to influence also the reactive wire resistance, which shows up as change in its so-called inner inductance. This inductance is normally negligible relative to the extrinsic inductance (Johnson and Graham, 2003) and is not included in (18).

The curves in Fig. 7, *b* are frequency dependences of wire resistance R_1 due to currents in the wire and in the earth, estimated using (17) for a standard geophysical copper wire. The earth-induced resistance increases proportionally to the first power of frequency. The skin effect in the wire becomes notable at a frequency about 10 kHz above which its contribution to resistance grows proportionally to the frequency square root. There are two essential points to note. First, the resistance due to earth currents depends on frequency but not on the resistivity of the subsurface. This is not surprising because if the current frequency in the line is fixed and the earth is electrically uniform, changes in its resistivity cause change to the distribution of induced current which adjusts to keep invariable the earth-induced resistance. In the case of a nonuniform (say, layered) earth, its contribution to the wire resistance depends on the resistivity distribution, but the earth in this study is assumed to be a uniform conductive half-space. Second, at frequencies above 10 kHz the contribution of the skin effect in the earth to the wire resistance is predominant, while the changes caused by R_{dc} and the skin effect in the wire are negligible.

Curves in Fig. 7, *c* obtained using (18) illustrate how the conductance L_1 depends on the current frequency and the resistivity of the earth. Increase in both frequency and conductivity only slightly decreases L_1: their change of six orders of magnitude causes a two-fold decrease at most.

The shunt conductance G depends on the insulation material (Johnson and Graham, 2003), and is 10^{-11} S/m for geophysical wires with intact insulation.

In order to check the above model, it is reasonable to compare first the model predictions with the responses measured at the midpoint of the wire perimeter (Fig. 2). The point $x = P/2$ was chosen because it was the point of maximum amplitude of the basic current standing waves. The wire inductance and resistance were estimated with (17) and (18) taking into account the skin effect in the wire and in the earth. According to VES and TEM data, the earth to depths of 200–250 m corresponds to a uniform half-space with resistivity ρ of a few hundreds of Ohm·m. The model curve in Fig. 8 was obtained for ρ = 500 Ohm·m.

As mentioned above, the capacitance C depends on many factors which are unknown a priori and elude precise estimation. The only possible solution is thus to assume some reasonable C value on the basis of (14) and then to improve it if necessary, i.e., it is a parameter to be fitted. For the case of Fig. 8 it was assumed to be $C = 4.7\cdot10^{-11}$ F/m.

The curve in Fig. 8 is a result of summation of 3000 terms of series (13), with a 1 ms period T of current pulses.

Although the measured and computed data are in a general agreement, the oscilaltion periods and attenuation rates differ notably. The period misfit, not very large, can be further reduced by fitting the capacitance. The amplitude of both experimental and model current oscillations decays exponentially, but oscillating current attenuates much faster in real loops than it is predicted by the loop model in the form of two identical transmission lines. Unlike period fitting, the case of attenuation is more complex for the lack of adjustable parameters in the model which would change the attenuation rate of the current standing waves. Mind that the resistance added due to the earth skin effect is independent of the earth resistivity (see above). The actual height of the wire above the ground likewise causes no influence on its resistance and inductance. Inductance, though depending on earth's resistivity (Fig. 7, *c*), cannot be used as a fitting parameter as the dependence is too weak.

Therefore, the chosen loop model appears to miss some essential point of the system though giving reasonable predictions. Which is this missing point?

Remember that the loop was assumed to be presented as a symmetrical combination of two identical transmission lines (Fig. 2, *b*, *c*). The point $x = P/2$ has the potential of the earth, i.e., same as at $x = 0$, and the processes in the two loop halves are thus expected to be independent of each other. The question is how far they are actually independent?

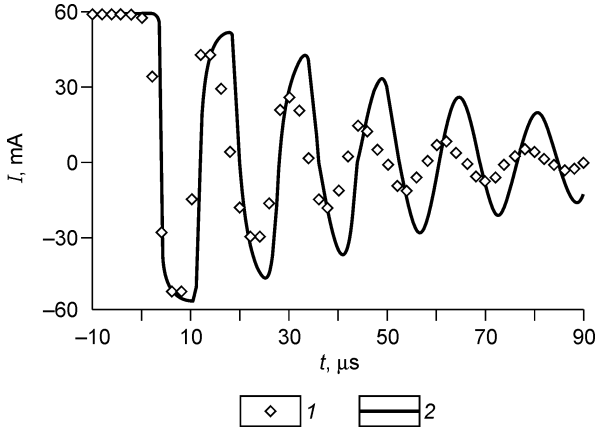

Fig. 8. Measured (*1*) and model (*2*) current oscillations at wire midpoint ($x = P/2$). Model oscillations computed with regard to effect of magnetic field of image current (Fig. 7, *a*) and skin effect in wire.

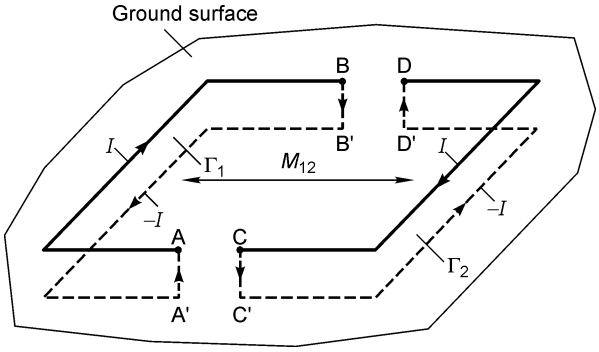

Fig. 9. Two transmission lines. There are two kinds of current in each line: forward current along the wire and its image in the earth flowing in the opposite sense. Transmission lines can be treated independently if largely spaced but, when approaching, they make up a system in which they experience mutual inductance to be taken into account in analysis.

See two transmission lines AB and CD in Fig. 9, each consisting of a wire and the underlying ground. Small bold circles mark the points where the wire is grounded; the input current sources are not shown for the sake of simplicity (Fig. 2, *b*).

Consider, for instance, the line AB on the left. Its per-unit-length parameters were calculated with regard to the effect of the underlying earth. There is forward current in the wire and the image return current through the earth, which makes up a closed circuit Γ_1. The magnetic flux produced by the image current is added to the wire magnetic flux to change its self inductance and self resistance. The wire inductance and resistance, with regard to skin effect in the earth and in the wire, are L_1^{AB} and R_1^{AB}, respectively. In the same way, forward current in the line CD returns through the earth along CC′D′D thus making the closed circuit Γ_2. With the magnetic field induced by the current along this circuit, the wire inductance and resistance are L_1^{CD} and R_1^{CD}. For identical lines and symmetrical earth $L_1^{AB} = L_1^{CD} = L_1$ and $R_1^{AB} = R_1^{CD} = R_1$.

In calculations for Fig. 8, the two lines were considered separately. However, if the lines are closely spaced, the circuits interact through the mutual inductance M_{12}. This inductive interaction should be included as the respective correction to the complex resistance of each line and, of course, of the loop as a whole.

Now imagine that the spacing between the lines becomes smaller, i.e., the point A approaches C and B approaches D. As the lines meet at these points, there appears a closed horizontal loop with the clockwise current *I*. At the same time, the earth currents, meeting at A′, C′ and B′, D′ make an image closed loop with counterclockwise current along it. This is apparently the response induced in the loop ABDC on the surface by the magnetic field of the image current A′B′D′C′ that is responsible for the Γ_1-Γ_2 mutual inductance correction to the loop complex resistance. Thus, one has to add L_2 and R_2 to L_1 and R_1 in (17) and (18).

The inductance L_2 and the resistance R_2 produced in the loop laid on the surface by the Γ_1-Γ_2 mutual inductance were estimated using an equation for the self-impedance $\dot{Z}_2$ of a circular loop of the radius *a* laid at the height *h* above a uniform half-space of the conductivity σ, with current in it of the angular frequency ω (Sobolev and Shkarlett, 1967):

$$\dot{Z}_2 = -\frac{6\cdot 10^{-7}\cdot \omega R}{\beta^2} e^{-3h/R}\left(3 - \sqrt{9 + 4j\beta^2}\right)^2, \quad (19)$$

where $\beta = a\sqrt{\omega\sigma\mu_0}$.

Correspondingly, the active resistance R_2 is

$$R_2 = \frac{\mathrm{Re}\dot{Z}_2}{P}, \quad (20)$$

and the inductance L_2 is

$$L_2 = \frac{\mathrm{Im}\dot{Z}_2}{j\omega P}. \quad (21)$$

It is noteworthy that (19) was obtained for a circular loop while the aim was to account for square loop transients. Equation (19) was applied presuming a known dependence of the loop self-impedance on the loop area. So, the self-impedance of a circular loop was calculated with its radius *a* chosen such that the loop were equal in area to a square loop of the side *A*: $a = A/\sqrt{\pi}$. For instance, for the 200×200 m^2 loop, the radius of the equivalent loop is 112.8 m ≈ 113 m.

See Figure 10 for frequency dependences of R_2 and L_2, those of earlier found $R_1(f)$ and $L_1(f)$ (Fig. 7, *b*, *c*), and total resistance *R* and inductance *L* with regard to (i) interaction of each loop half with its image current, (ii) their mutual inductance, and (iii) skin effect in the wire.

Taking into account the interaction of the two transmission lines (Fig. 9), at least with (19), appears to cause only slight changes to their parameters (Fig. 10). To see what has actually happened, the plots of current measured at three loop points (Fig. 4) are superposed in Fig. 11 with the computed dependences $I(t)$ in which L_2 and R_2 found according to (20) and (21) are added to the previously obtained inductance (L_1) and resistance (R_1). Then it becomes obvious that the mutual inductance correction improves substantially the fit between the measured and computed current attenuation rates.

Discussion

It is pertinent to detail some features of the above model and modeling results. Equation (19) was applied with an assumption which needs a comment. At high frequencies a loop is a distributed circuit, and at early times the current changes along the loop wire (see above and also Helwig and Kozhevnikov, 2003; Kozhevnikov, 2006; Kozhevnikov and Nikiforov, 1998, 2000). However, (19) was derived for a loop simulated by a lumped circuit, i.e., neglecting the delay in the wire–earth system. This assumption ensures an accuracy acceptable in engineering applications within a bandwidth corresponding to the quasi-static approximation (Sobolev and Shkarlett, 1967), but it is never possible to estimate a priori how much the inductance and resistance caused by mutual

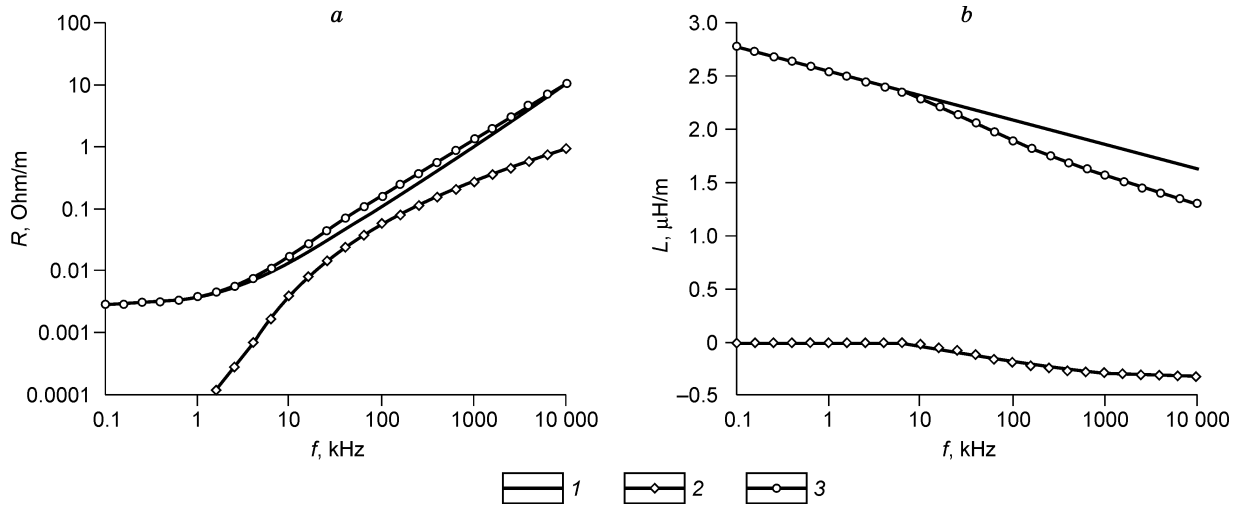

Fig. 10. Frequency-dependent resistance (*a*) and inductance (*b*). *1*. Without regard to mutual inductance between lines (R_1, L_1). *2*. Due to mutual inductance between lines (R_2, L_2). *3*. With regard to all effects (R, L).

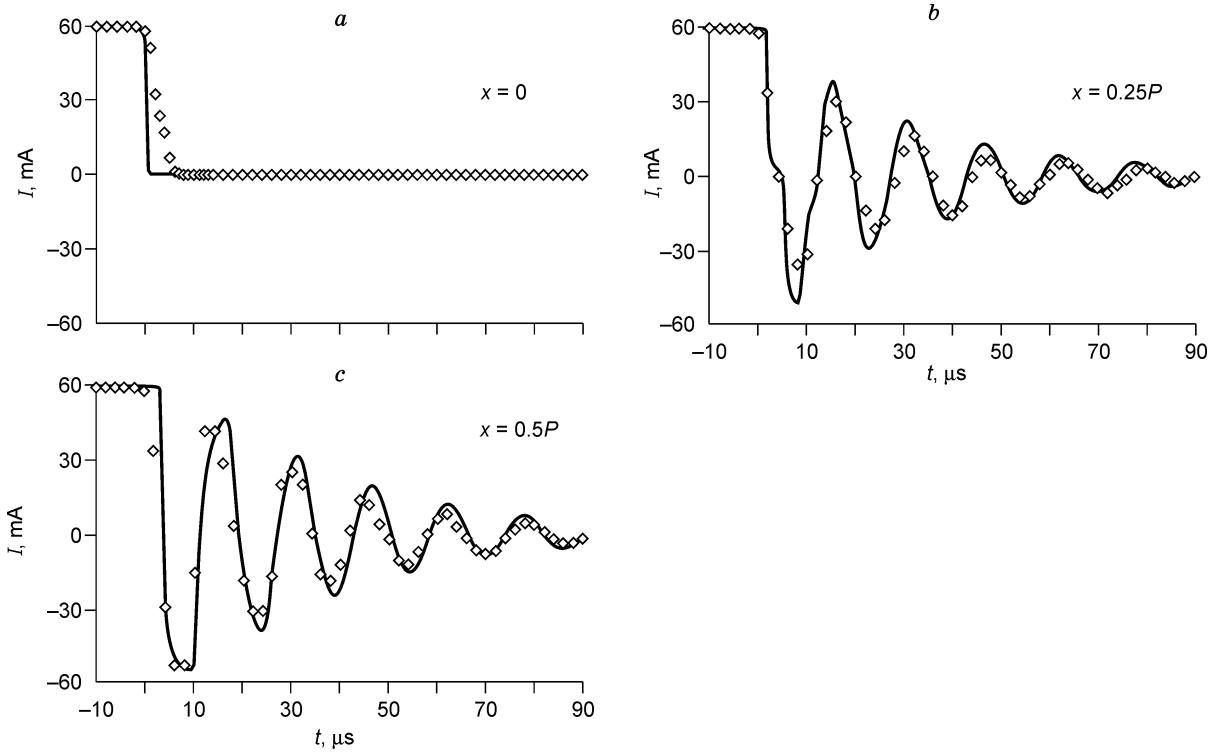

Fig. 11. Measured and model current oscillations at different points of loop wire. Unlike those in Fig. 8, model data are computed with regard to mutual inductance between lines. Symbols same as in Fig. 8.

inductance between two halves of a real loop (Fig. 9) would differ from those calculated with (20) and (21). The only thing one can do with this is to use (20) and (21) as some approximation and to look at the result, which appears to be more than satisfactory.

Note that if one tried to account for the attenuation of current oscillations uniquely with the resistance added to the loop self-resistance due to mutual inductance between its halves, the calculated decay would be three times faster than the measured one. Thus, at the loop resonance frequency two thirds of the induced resistance is that of the transmission line consisting of the wire and the underlying ground.

When comparing the experimental and theoretical responses in Fig. 11, *a*, one may wonder why the current turn-off measured at the input (x = 0) takes 5 μs instead of being instant as predicted by the theory. There must be several reasons. They are, first, the features of the electronic switch which disconnects the loop input from a battery in a very short but finite time; second, common-mode capacitive pickup at the input of the oscilloscope employed to record the signals.

This pickup has the largest effect on measurements near the loop input where voltage is in antinode (Fig. 3, *b*); third, approaching the loop input where additional devices are connected, one may expect ever greater departure of the wire–earth system from the chosen uniform transmission-line model. Exhaustive analysis of the wire–earth system requires general methods of which the finite-element method (Wang and Liu, 2001) is likely the most promising one.

Correction for the mutual inductance of two loop lines provides a better fit between measured and computed attenuations of the current standing waves and, more so, accounts for the known (Vakhromeev et al., 1991) dependence of characteristic decay time on earth's resistivity. As noted above, the attenuation of loop current depends most strongly on resistance due to the skin effect in the earth (Fig. 10), which, however, is independent of earth resistivity. On the other hand, the additional resistance caused by the interaction of two lines, though contributing less to the linear wire resistance, does depend on earth's resistivity, and this dependence, at least in principle, allows one to apply inversion of loop current oscillations for estimating the resistivity of shallow ground. Not going far into details of the inversion issue, note that the best fit between theory and measurements for the data of Fig. 10 was at $\rho = 500$ Ohm·m. This value found through fitting to range between 10^2 and 10^3 Ohm·m is close to the local resistivity estimated from VES and TEM data.

According to fitting results, ρ controls both the attenuation and the period of current oscillations. This is because earth's resistivity influences current distribution in the earth and thus the wire inductance *L* which, in turn, affects the velocity of EM waves in the wire–earth transmission line and, correspondingly, the frequency of the current and voltage standing waves in each line after it has been switched-off from the battery.

For period one may use another fitting parameter besides ρ, the capacitance *C* of the line which, along with inductance, controls the propagation constant influencing the velocity of EM waves in the line. Mind that the wire capacitance depends on many hardly predictable factors. The "best" *C* obtained by fitting is rather an effective parameter impossible to calculate a priori. There is another point to mention in this respect. Before applying the mutual inductance correction, capacitance fitting was tried to improve the period fit between the measured and computed transients, which was successful either at early or at late times but never throughout the time range. The period fit at all times was achieved after the correction (Fig. 11, *b*, *c*), which also provided account for the measured current attenuation rate.

Thus, the per-unit-length wire parameters that enter equation (9) should include the correction $\dot{Z}_2$ for the mutual inductance of the loop halves.

Conclusions

At early times, the wire of an ungrounded horizontal loop in combination with the underlying shallow subsurface behaves as a transmission line in which current turn-off is governed by the wave equation.

The current turn-off in the wire–earth system can be simulated as a superposition of waves of different wavelengths and frequencies that travel in forward and back directions and reflect from the loop ends and from the midpoint.

Shunting the loop by a resistor with its resistance equal to the double characteristic impedance of the wire–earth transmission line provides matching for current waves traveling from the midpoint to the loop input. As a result, no ringing arises and the relaxation time becomes equal to the half-period of current oscillations in the loop at its resonant frequency.

An ungrounded horizontal loop is asymmetrical at early times, and its primary magnetic field differs from that predicted by the conventional EM methods.

The per-unit-length parameters of the wire–earth line (*R*, *L*, *C*, and *G*) show an intricate dependence on earth's resistivity and frequency (and/or time), which makes solving the wave equation quite difficult.

Current turn-off in an ungrounded horizontal loop was explored applying the theory of transmission lines by simulating the loop as a symmetrical combination of two identical transmission lines with shorted outputs.

With this approach, the problem becomes easy to solve even in the case of frequency and resistivity dependence of the line parameters. Modeling was performed in the frequency domain with subsequent transformation into the time domain.

Comparison of measured and computed decays of current standing waves in the loop showed that good fit requires taking into account (1) interaction of each transmission line in the loop with its own image current, (2) mutual inductance of the two lines, and (3) skin effect in the wire.

As a result of mutual inductance, the transmission lines have their parameters—and, hence, the parameters of the whole loop—depending on earth's conductivity, which, at least in principle, may allow one to infer the earth resistivity from loop high-frequency responses.

The manuscript profited much from constructive criticism by the reviewers A.K. Zakharkin and V.S. Mogilatov.

References

Alekseev, E.P., Yakovlev, A.V., 1982. Time-domain measurements of electrical parameters of feedlines. Geofizicheskaya Apparatura. Issue 75, 29–35.

Alekseev, E.P., Veshev, A.V., Yakovlev, A.V., 1978. Measurements of electrical parameters and operation of feedlines in EM surveys. Geofizicheskaya Apparatura. Issue 66, 49–58.

Aramanovich, I.G., Levin, I.I., 1969. Equations of Mathematical Physics [in Russian]. Nauka, Moscow.

Baskakov, S.I., 1980. Radio Circuits with Distributed Elements [in Russian]. Vysshaya Shkola, Moscow.

Bazutkin, V.V., Dmokhovskaya, L.F., 1983. Calculations for Transient Processes and Overvoltage [in Russian]. Energoatomizdat, Moscow.

Efimov, F.D., 1976. Transient self response of a receiver coil and its effect on loop-loop TEM measurements, in: Sedov, M.P. (Ed.), Geophysical Prospecting Methods. Resistivity Surveys [in Russian]. NPO "Geofizika", Issue 26, pp. 72–79.

Evdokimov, R.V., Savel'ev, N.N., Maryarevskii K.V., 1974. Feedline tuning in the method of infinitely long cable (ILC). Geofizicheskaya Apparatura, Issue 55, 64–71.

Hayles, J.G., Sinha, A.K., 1986. A portable local loop VLF transmitter for geological fracture mapping. Geophysical Prospecting 34, 873–896.

Helwig, S.L., Kozhevnikov, N.O., 2003. Schwingungen in TEM Sendesignalen zu frühen Zeiten, in: Hördt, A., Stoll, J.B. (Eds.), 20 Kolloquium Elektromagnetische Tiefenforschung, Königstein, 29.09–03.10.2003, pp. 11–20.

Johnson, H., Graham, M., 2003. High-speed Signal Propagation. Advanced Black Magic. Prentice-Hall, New Jersey.

Kozhevnikov, N.O., 2006. An ungrounded horizontal loop as a system with distributed elements. Geofizika, No. 1, 29–39.

Kozhevnikov, N.O., Nikiforov, S.P., 1998. Distributed EM parameters of an ungrounded horizontal loop and their relation to the near-surface geoelectrical features, in: Application of Geophysics to Engineering and Environmental Problems, Proc. Symp., EEGS, Chicago, pp. 1019–1027.

Kozhevnikov, N.O., Nikiforov, S.P., 2000. Early time TEM response of an ungrounded horizontal loop—a new look, in: Expanded Abstracts, 62nd EAGE Conference, Glasgow, D-ll.

Kozhevnikov, N.O., Plotnikov, A.E., 2004. Estimating the potentialities of the TEM method for studying shallow ground. Geofizika, No. 6, 33–38.

Lavrov, G.A., Knyazev, A.S., 1965. Subsurface and Near-Surface Antennas [in Russian]. Sovetskoe Radio, Moscow.

Nakhabtsev, A.S, Sapozhnikov, B.G., Yabluchanskii, A.I., 1985. Resistivity Surveys with Ungrounded Wires [in Russian]. Nedra, Leningrad.

Nikolaev, Yu.V., Sidorov, V.A., Tkachenko, A.K., 1988. Coincident-Loop Self Responses in TEM Soundings [in Russian]. Moscow, Dep. VINITI 04.04.08, No. 2563–V88.

Qian, B., 1985. Selection of frequency bandwidth of a TEM receiving system to avoid false anomalies. Geoexploration 23, 519–526.

Simonyi, K., 1956. Teoretische Elektrotechnik. Deutscher Verlag der Wissenschaften, Berlin.

Sobolev, B.C., Shkarlett, Yu.M., 1967. Attachable and Screen Sensors (for Vortex Current Control) [in Russian]. Nauka, Novosibirsk.

Sokolov, V.P., Tabarovskii, L.A., Rabinovich, B.I., 1978. Transformation of TEM responses measured with current pulses of non-ideal waveforms, in: Sokolov, V.P. (Ed.)., Electromagnetic Fields in Exploration Geophysics: Theory and Practice [in Russian]. IGG SO RAN, Novosibirsk, pp. 81–92.

Vakhromeev, G.S., Kozhevnikov, N.O., Nikiforov, S.P., Nikitin, I.V., 1991. A method of resistivity surveys. Patent No. 16995248. Published in Byulleten' Izobretenii.

Veshev, A.V., 1980. DC and AC Resistivity Surveys [in Russian]. Nedra, Leningrad.

Veshev, A.V., Yakovlev, A.V., Sapozhnikov, B.G., 1974. Equivalent circuits and parameters of receiver lines. Geofizicheskaya Apparatura, Issue 55, 46–56.

Vishnyakov, A.E., Vishnyakova, K.A., 1974. Excitation and Measurement of Fields in Resistivity Surveys [in Russian]. Nedra, Leningrad.

Wang, Yaw-Juen, Lui, Shi-Jie, 2001. A review of methods for calculation of frequency-dependent impedance of overhead power transmission lines. Proc. Natl. Sci. Counc. ROC(A) 25 (6), 329–338.

Zakharkin, A.K., 1981. Near-Field TEM Method of Resistivity Surveys with TZIKL Instruments: Methodological Guide [in Russian]. SNIIGGiMS, Novosibirsk.

Editorial responsibility: M.I. Epov